

# Real-Time Congestion Pricing Strategies for Toll Facilities

Jorge A. Laval<sup>a,\*</sup>, Hyun W. Cho<sup>a</sup>, Juan C. Muñoz<sup>b</sup>, Yafeng Yin<sup>c</sup>

<sup>a</sup>*School of Civil and Environmental Engineering, Georgia Institute of Technology*

<sup>b</sup>*Department of Transport Engineering and Logistics, Pontificia Universidad Católica de Chile*

<sup>c</sup>*Department of Civil and Coastal Engineering, University of Florida*

---

## Abstract

This paper analyzes the dynamic traffic assignment problem on a two-alternative network with one alternative subject to a dynamic pricing that responds to real-time arrivals in a system optimal way. Analytical expressions for the assignment, revenue and total delay in each alternative are derived as a function of the pricing strategy. It is found that minimum total system delay can be achieved with many different pricing strategies. This gives flexibility to operators to allocate congestion to either alternative according to their specific objective while maintaining the same minimum total system delay. Given a specific objective, the optimal pricing strategy can be determined by finding a single parameter value in the case of HOT lanes. Maximum revenue is achieved by keeping the toll facility at capacity with no queues for as long as possible. Guidelines for implementation are discussed.

*Keywords:* system optimum, user equilibrium, congestion pricing

---

## 1. Introduction

There are currently more than a dozen cities around the world that implement zone- or cordon-based congestion pricing, and around 20 toll facilities in the United States subject to congestion pricing. The pricing strategies in these facilities are inspired by the “first-best toll” concept borrowed from the economics literature, which can be stated as “System Optimum (SO) will be equivalent to User Equilibrium (UE) with tolls derived from the SO solution” (see e.g. Carey and Watling, 2012). This concept has been adapted to the

---

\*Corresponding author. Tel. : +1 (404) 894-2360; Fax : +1 (404) 894-2278

*Email address:* [jorge.laval@ce.gatech.edu](mailto:jorge.laval@ce.gatech.edu) (Jorge A. Laval) *Preprint submitted to Transportation Research Part B* September 24, 2014

30 case of traffic flow rather directly, and it is our view that some important  
31 traffic dynamics properties may have been overlooked in doing so.

32 Although there are a number of studies examining the performance of  
33 High Occupancy Toll (HOT) lanes (see, e.g. Supernak et al., 2003, 2002a,b;  
34 Burris and Stockton, 2004; Zhang et al., 2009)) and travelers' willingness to  
35 pay (Li, 2001; Burris and Appiah, 2004; Podgorski and Kockelman, 2006;  
36 Zmud et al., 2007; Finkleman et al., 2011), SO tolling policies have received  
37 little attention. Existing studies focused on ad-hoc objectives that the tolling  
38 agencies may seek to achieve, such as ensuring free-flow conditions on HOT  
39 lane. For example, Li and Govind (2002) developed a toll evaluation model  
40 to assess the optimal pricing strategies of the HOT lane that can accomplish  
41 different objectives such as ensuring a minimum speed on the HOT lane, or  
42 in the general-purpose lanes (GPL), or maximizing toll revenue. Zhang et al.  
43 (2008) proposed the logit model to estimate dynamic toll rates of the HOT  
44 lane after calculating the optimal flow ratios by using feedback-based algo-  
45 rithm on the basis of keeping the HOT lane speed higher than 45mph. Yin  
46 and Lou (2009) explored two approaches including feedback and self-learning  
47 methods to determine dynamic pricing strategies for the HOT lane, and the  
48 comparative results showed that the self-learning controller is superior to  
49 the feedback controller in view of maintaining a free-flow traffic condition  
50 for managed lanes. Lou et al. (2011) further developed the self-learning ap-  
51 proach in Yin and Lou (2009) to incorporate the effects of lane changing  
52 using the hybrid traffic flow model in Laval and Daganzo (2006). Burris  
53 et al. (2009) examined the potential impacts of different tolling strategies on  
54 carpools, which includes removing or reducing the preferential treatment for  
55 them in the HOV lane.

56 In our formulation the social cost to be minimized is total system delay,  
57 and does not include the effects that tolls may have on trip generation or  
58 departure-time choice. The proposed pricing strategies are real-time, in the  
59 sense that they respond to real-time traffic arrivals in a way that minimizes  
60 total system delay for that particular rush hour. Therefore, the underlying  
61 assumption is that demand is inelastic within the day, but it could very  
62 well be elastic from day to day. In this context, this paper proposes a real-  
63 time pricing mechanism that is consistent with known properties of marginal  
64 costs under inelastic demands, i.e.: the cost of adding an additional user to  
65 a specific alternative is given by the time until congestion clears, it is not  
66 well defined when capacity is reached, and the SO assignment is not unique  
67 (Muñoz and Laval, 2005; Kuwahara, 2007). Towards this end, this paper is

68 organized as follows. Section 2 presents the problem formulation along with  
69 the SO and UE solutions. Section 3 summarizes the general properties of SO  
70 tolls, including expressions for delays and revenue. Section 4 examines the  
71 special case of HOT lanes, and finally section 5 presents a discussion.

## 72 2. Problem Formulation

73 Consider the equilibrium between two alternatives with finite capacity,  
74 one of which is priced. To fix ideas, we take the example of a Managed Lane  
75 (ML) competing with the general-purpose lanes (GPL), but the formulation  
76 to be developed also applies to other cases such as toll roads or zone-based  
77 pricing. Our focus is on real-time pricing strategies and therefore we do not  
78 assume that traffic demand is known in advance, but only as it realizes.

79 Let  $A(t)$  be the cumulative number of vehicles at time  $t$  that have entered  
80 a freeway segment containing a ML entrance, and let the corresponding flow  
81 be  $\lambda(t) = \dot{A}(t)$ . All vehicles are bound for a single destination past a GPL  
82 bottleneck of capacity  $\mu_0$ , which may be bypassed by paying a toll  $\pi(t)$  upon  
83 entering the ML at time  $t$ , which has a bottleneck of capacity  $\mu_1$ ; see Fig. 1.

84 The cumulative count curve of vehicles using route  $r$  ( $r=0$  for the GPL  
85 and  $r = 1$  for the ML) is denoted  $A_r(t)$  and the flow,  $\lambda_r(t) = \dot{A}_r(t)$ . Clearly,

$$86 \quad \lambda(t) = \lambda_0(t) + \lambda_1(t), \quad (1)$$

87 and is assumed unimodal. Let  $\tau_r(t)$  be the trip time in route  $r$  experienced  
88 by a user arriving at time  $t$ :

$$89 \quad \tau_r(t) = \tau_r + w_r(t), \quad (2)$$

90 where  $\tau_r$  is the free-flow travel time, and  $w_r(t)$  is the queuing delay, which  
91 can be expressed as:

$$92 \quad w_r(t) = \frac{A_r(t) - A_r(t_r)}{\mu_r} - (t - t_r), \quad t_r < t < T_r, \quad (3)$$

93 where  $t_r$  and  $T_r$  represent the times when route  $r$  begins and ends being  
94 congested, respectively. Let:

$$95 \quad \Delta = \tau_0 - \tau_1 \quad (4)$$

96 be the extra free-flow travel time for using the free alternative. Although  
97 in many cases one would expect  $\tau_0 \approx \tau_1$ , this will not be assumed here for

98 maximum generality. To simplify the exposition, we assume that  $\Delta > 0$   
 99 hereafter; the other two cases will be discussed in the last section of this  
 100 paper. Under this assumption, we will see that  $t_1 < t_0$  in the SO solution,  
 101 i.e. the ML is used at capacity before the GPL, as shown next.

### 102 2.1. System Optimum

103 The SO solution to our problem (without pricing) is presented in Fig. 2,  
 104 which shows the system input-output diagram using total arrivals  $A(t) =$   
 105  $A_0(t) + A_1(t)$  and total virtual departures  $D^*(t)$ .<sup>1</sup> The area between these  
 106 curves is the total system delay, i.e. the total time spent queuing in the  
 107 system. The method to obtain the curve  $D^*(t)$  was introduced in Muñoz  
 108 and Laval (2005), and is best visualized by imagining a ring connected to the  
 109 rightmost end of  $D^*(t)$  that is slid along  $A(t)$  from right to left until  $D^*(t)$   
 110 “touches”  $A(t)$  again (at point “1” in the figure). This point corresponds  
 111 to the time when both alternatives start being used at capacity ( $t_0$  in our  
 112 case since  $\Delta > 0$ , and  $\lambda(t_0) = \mu_0 + \mu_1$ ), and from here one can identify  
 113 the arrival time of the last vehicles to experience delay in each alternative,  
 114  $T_r, r = 0, 1$ , and the time when the shorter alternative starts being used at  
 115 capacity, ( $t_1$  in our case, and  $\lambda(t_1) = \mu_1$ ); see Fig. 2. This figure also shows  
 116 how to obtain the total system departure curve  $D(t)$ , which gives the count  
 117 of vehicles reaching the destination at time  $t$ . Notice that total arrivals and  
 118 departures in the system are not first-in-first-out. The resulting flow pattern  
 119 is summarized below (Muñoz and Laval, 2005):

120  
 121 *System Optimum Conditions:* The SO assignment when  $\Delta > 0$  for users  
 122 arriving at  $t$  satisfy:

- 123 1.  $0 \leq t \leq t_1$ : everybody uses the ML
- 124 2.  $t_1 \leq t \leq t_0$ : the ML is used at capacity, excess inflow uses the GPL
- 125 3.  $t_0 \leq t \leq T_0$ : both alternatives are used at capacity
- 126 4.  $t \geq T_0$ : everybody uses the ML □

127 Notice that in  $t_0 \leq t \leq T_0$  the solution in terms of the alternative-specific  
 128 arrivals  $A_r(t), r = 0, 1$  is not unique. This is because the SO conditions simply  
 129 state that within this time interval both alternatives be used at capacity.

---

<sup>1</sup>Virtual departures are defined as the arrival curve shifted to the right by the free-flow travel time.

130 Where to store the queues is up to the operator. Therefore, hereafter we  
 131 focus on  $t_0 \leq t \leq T_0$  because it is the only time interval where we have  
 132 flexibility to define  $A_r(t)$ . Without loss of generality and for simplicity we  
 133 also set  $t_0 = 0, A(t_0) = 0$ . This implies that the delay to users arriving in  
 134  $t < t_0$  will not be considered. But this is irrelevant because such a delay is a  
 135 constant of our problem, i.e. independent of the pricing strategy.

136 Setting  $t_0 = 0, A(t_0) = 0$  simplifies the construction of total arrivals and  
 137 departures, as shown in Fig. 3a, and streamlines the derivation of alternative-  
 138 specific input-output diagrams in Figs. 3b,c, which are first-in-first-out. Re-  
 139 call that arrivals  $A_r(t)$  are not unique; the only requirement is that they  
 140 start at the origin, remain above the virtual departures, and pass through  
 141 points “1” and “2” in Figs. 3b,c, respectively. The departure curves at each  
 142 alternative measured at the destination,  $D_r(t)$ , are obtained by shifting the  
 143 virtual departures by the free-flow travel time  $\tau_r$ ; total system departures are  
 144 then  $D(t) = D_0(t) + D_1(t)$ .

145 The total system cost is the area between total arrivals and departures,  
 146 which can be partitioned into the three components shown in Fig. 3a: (i)  
 147 the total delay defined previously (area 0-4-3-0), (ii) the fixed travel time  
 148  $\tau_1$  incurred by all users (striped area), and (iii) the extra travel time  $\Delta\mu_0 T_0$   
 149 incurred by GPL users (lightly shaded area). The reader can verify that  
 150 the striped and lightly shaded areas in Fig. 3a correspond to the sum of the  
 151 respective areas in parts b and c of the figure.

152 Figs. 3b,c also show the delay, travel time and externality in each alter-  
 153 native,  $w_r(t), \tau_r(t)$  and  $e_r(t)$ , respectively. It can be seen that:

$$154 \quad e_r(t) = T - t - \tau_r(t). \quad (5)$$

155 The marginal cost  $\tau_r(t) + e_r(t)$  in each alternative gives the extra cost incurred  
 156 by the system if an additional unit of flow uses such alternative. In  $t_0 \leq t \leq$   
 157  $T_0$  the marginal cost is given by the time remaining until the end of congestion  
 158 in the system, and it is identical on both alternatives, as expected. Outside  
 159 this time interval only the alternative with the least marginal cost (ML in  
 160 this case) is used.

161 It is worth noting that point “2” in Fig. 3c implies that at  $T_0$  there has to  
 162 be a queue in the ML, and therefore completely eliminating queues from the  
 163 ML facility is not system optimal (when  $\Delta > 0$ ). The reason is that starting  
 164 at this time the GPL must not be used since its marginal cost is greater than  
 165 the ML marginal cost.

166 *2.2. User Equilibrium with pricing*

167 The UE condition for our problem under any pricing strategy  $\pi(t)$ —not  
 168 necessarily SO tolls—can be expressed as

$$169 \quad \tau_0(t) = \tau_1(t) + \pi(t) \quad (6)$$

170 when both alternatives are used; otherwise, only the less expensive alterna-  
 171 tive is used. Notice that in this formulation the toll has units of time, and  
 172 implies that all users have the same value of time. The case of heterogeneous  
 173 users is discussed in section 5.

174 Following Laval (2009) it is more convenient to express the UE condition  
 175 (6) in differential form, which equalizes the rate of change in travel cost  
 176 among alternatives, i.e.  $\dot{\tau}_0(t) = \dot{\tau}_1(t) + \dot{\pi}(t)$ , with  $\dot{\tau}_r(t) = \dot{w}_r(t) = \lambda_r(t)/\mu_r -$   
 177  $1, r = 0, 1$  by (3). This gives in our case:

$$178 \quad \rho_0(t) = \rho_1(t) + \dot{\pi}(t), \quad (7)$$

179 where we have defined the demand-capacity ratios  $\rho_r(t) = \lambda_r(t)/\mu_r, r =$   
 180  $0, 1$ . Notice that the differential UE condition is applicable only when the  
 181 initial condition is in UE equilibrium. Substituting (1) into (7) gives the UE  
 182 assignment when both alternatives are used:

$$183 \quad \rho_0(t) = \rho(t) + \bar{\mu}_1 \dot{\pi}(t), \quad (8a)$$

$$184 \quad \rho_1(t) = \rho(t) - \bar{\mu}_0 \dot{\pi}(t), \quad (8b)$$

186 where  $\mu = \mu_0 + \mu_1, \bar{\mu}_r = \mu_r/\mu$  and  $\rho(t) = \lambda(t)/\mu$  is the system demand-  
 187 capacity ratio. It can be seen that for constant or no tolls ( $\dot{\pi}(t) = 0$ ) the  
 188 UE condition implies that each alternative and the system have the same  
 189 demand-capacity ratio. Arrival curves are obtained by integrating (8) from  
 190 the time when both alternatives start being used, say  $t_{ini}$ , and thus:

$$191 \quad A_r(t) = (-1)^r \bar{\mu}_0 \mu_1 (\pi(t) - \pi(t_{ini})) + \bar{\mu}_r A(t), \quad r = 0, 1. \quad (9)$$

192 where we have used  $A(t_{ini}) = 0$  without loss of generality.

193 **3. Properties of System Optimum tolls**

194 In this section we identify and examine the properties of the SO toll,  $\pi(t)$ ,  
 195 that produces a SO assignment under UE. The goal of SO tolls is for every

196 user to perceive the marginal cost it imposes to the system. This could be  
 197 accomplished in our case by charging the externality in each alternative given  
 198 by (5). Equivalently, since we want to maintain the GPL toll-free we will  
 199 charge the difference in the externalities to the ML only. This is illustrated  
 200 in Fig. 4a, which shows the marginal cost in equilibrium along with travel  
 201 times, delays, and externalities on each alternative, as a function of time.  
 202 The figure also shows the SO flow pattern in each relevant time interval,  
 203 with the exception of  $t_0 \leq t \leq T_0$ , where SO flows are not unique, and nor  
 204 are  $\tau_r(t)$  and  $e_r(t)$ . It follows that in  $t_0 \leq t \leq T_0$  the toll  $\pi(t)$  is also not  
 205 unique and can be chosen freely but within the following constraints:

206 (i) boundary conditions constraints:

$$207 \quad \pi(t_0) = \Delta, \quad \pi(T_0) = \Delta - w_1(T_0), \quad \text{and} \quad (10a)$$

208 (ii) active bottleneck constraints:

$$209 \quad \dot{\pi}(t) \geq (\mu - \lambda(t))/\mu_1, \quad \text{if GPL at capacity with no queue} \quad (10b)$$

$$210 \quad \dot{\pi}(t) \leq (\lambda(t) - \mu)/\mu_0, \quad \text{if ML at capacity with no queue} \quad (10c)$$

$$211 \quad -\lambda(t)/\mu_1 \leq \dot{\pi}(t) \leq \lambda(t)/\mu_0, \quad \text{if GPL and ML have queues} \quad (10d)$$

213 The boundary condition constraints (10a)–depicted as points “1” and “2”  
 214 in Fig. 4b—are a consequence of the SO conditions in the time intervals  $t \leq t_0$   
 215 and  $t \geq T_0$ , which force pricing to be either fixed or arbitrary. Before  $t_1$  there  
 216 is no congestion and therefore as long as  $\pi(t) \leq \Delta$  all drivers will choose the  
 217 ML, as required by the SO condition. This is shown in Fig. 4b by the shaded  
 218 rectangles, which indicates that the toll could be anywhere inside this area.  
 219 During the time interval  $t_1 \leq t \leq t_0$  the ML has to operate at capacity with  
 220 no queues while the excess demand should be diverted to the GPL, which is  
 221 achieved using  $\pi(t) = \Delta$ . After  $T_0$  only the ML should be used, which can  
 222 be achieved, again, by pricing within the shaded area in the figure.

223 The active bottleneck constraints (10b), (10c) and (10d) ensure that the  
 224 bottlenecks will be used at capacity in  $t_0 \leq t \leq T_0$  and under all situations. In  
 225 particular, if there is no queue on alternative  $r$  one should impose  $\lambda_r(t) \geq \mu_r$   
 226 in (8a) or (8b), which gives (10b) or (10c). If there is a queue on both  
 227 alternatives, the less restrictive condition  $\lambda_r(t) \geq 0$  should be imposed, which  
 228 gives (10d).

### 229 3.1. Delays

230 The total delay for users arriving in  $t_0 \leq t \leq T_0$ ,  $W = \int_{t_0}^{T_0} (A(t) - \mu t) dt$ ,  
 231 is a constant in our problem and is given by the dark shaded area in Fig. 3a.

232 The delay in each alternative,  $W_r(\pi) = \int_{t_0}^{T_0} (A_r(t) - \mu_r t) dt$ , are functions of  
 233 the pricing strategy. Using (9) gives:

$$234 \quad W_r(\pi) = \int_{t_0}^{T_0} (-1)^r \bar{\mu}_0 \mu_1 (\pi(t) - \Delta) + (\bar{\mu}_r A(t) - \mu_r t) dt, \quad (11a)$$

$$235 \quad = (-1)^r \bar{\mu}_0 \mu_1 \int_{t_0}^{T_0} (\pi(t) - \Delta) dt + \bar{\mu}_r W \quad (11b)$$

236

237 where one can see that  $W = W_0(\pi) + W_1(\pi)$ , as expected. It is interesting  
 238 to note that manipulation of (11b) gives

$$239 \quad W_0(\pi)/\mu_0 - W_1(\pi)/\mu_1 = \int_{t_0}^{T_0} (\pi(t) - \Delta) dt, \quad (12)$$

240 which can also be verified in Fig. 4a: the shaded areas correspond to  $\int_{t_0}^{T_0} w_r(t) dt =$   
 241  $\int_{t_0}^{T_0} \mu_r w_r(t) dt / \mu_r = W_r / \mu_r$ ,  $r = 0, 1$ , respectively.

### 242 3.2. Revenue

243 Let  $R(\pi)$  be the revenue under strategy  $\pi(t)$ . It can be expressed as  
 244  $\int_{t_0}^{T_0} \lambda_1(t) \pi(t) dt$ , which by (8b) is also:

$$245 \quad R(\pi) = \bar{\mu}_1 \int_{t_0}^{T_0} \lambda(t) \pi(t) dt - \bar{\mu}_0 \mu_1 \int_{t_0}^{T_0} \dot{\pi}(t) \pi(t) dt, \quad (13a)$$

$$246 \quad = \bar{\mu}_1 \int_{t_0}^{T_0} \lambda(t) \pi(t) dt - C \quad (13b)$$

247

248 where  $C = \bar{\mu}_0 \mu_1 (\Delta^2 - (\Delta - w_1(T_0))^2) / 2$  is a constant that follows from  
 249  $\int_{t_0}^{T_0} \dot{\pi}(t) \pi(t) dt = \frac{1}{2} \pi^2(t) \Big|_{t_0}^{T_0}$  and (10a). Therefore, maximizing revenue can be  
 250 expressed as the following mathematical program:

$$251 \quad \max_{\pi(t)} \int_{t_0}^{T_0} \lambda(t) \pi(t) dt, \quad \text{subject to (10),} \quad (14)$$

252 and we have the following result:

253 **Result 3.1.** (Maximum Revenue) *Revenue is maximized for the highest possible*  
 254  *$\pi(t)$  that does not violate the SO condition; i.e., the ML is maintained*  
 255 *at capacity with no queues for as long as possible (see Fig. 5a).*



256 **Proof** Maximizing  $\int_{t_0}^{T_0} \lambda(t)\pi(t)dt$  is equivalent to maximizing  $\int_{t_0}^{T_0} \pi(t)dt$  be-  
257 cause (i)  $\lambda(t)$  is exogenous and nonnegative, and (ii) the active bottleneck  
258 constraints are in terms of  $\dot{\pi}(t)$ , which means that the highest possible  $\pi(t)$   
259 value at a given time  $t$  is obtained only if it is preceded by the highest pos-  
260 sible  $\pi(t')$  value at an earlier time  $t'$ . Therefore, the optimal solution can be  
261 obtained in a  $(t, \pi)$  diagram starting from each boundary point  $(t_0, \Delta)$  and  
262  $(T_0, \Delta - w_1(T_0))$ , and drawing curves of maximum slope from each one in the  
263 direction of increasing and decreasing time, respectively, until they cross, say  
264 at time  $t^*$ . This is shown in Fig. 5b, where these points have been labeled “1”  
265 and “2”, respectively. It can be seen that maximum slopes are constrained  
266 by (10c) and (10d), respectively, because at  $t = t_0$  there is no ML queue, and  
267 right before  $t = T_0$  there is a queue on both alternatives. It follows that in  
268  $t_0 \leq t \leq t^*$  the ML is maintained at capacity with no queues, and in  $t > t^*$   
269 a queue on both alternatives is allowed.  $\square$

270 Intuitively, from (12) one can see that maximizing  $\int_{t_0}^{T_0} \pi(t)dt$  also maximizes  
271 the difference  $W_0(\pi)/\mu_0 - W_1(\pi)/\mu_1$ , which is obtained by imposing the high-  
272 est and the lowest possible travel time to the GPL and ML, respectively.

### 273 3.3. Social benefits of SO tolls

274 The benefits of SO tolling compared to no tolling can also be quantified.  
275 Fig. 6 presents the input-output diagram in Fig. 3a, which assumes  $\Delta > 0$ ,  
276 along with the total departure curve assuming no tolls, namely  $D_{\pi=0}(t)$ . The  
277 details for obtaining this curve are omitted here in the reader is referred to  
278 Laval (2009). It can be seen that the social (i.e., delay) benefits of SO pricing  
279 is bounded by  $(T - \tau_0)\Delta\bar{\mu}_1$ . To see this, we note that the extra travel time  
280 with no tolls is bounded by  $\Delta\bar{\mu}_1$ , which is a tight bound when the slope  
281 between the origin and point “1” in the figure is  $\mu$ .

## 282 4. HOT lanes under linear tolls

283 System optimum tolls on HOT lanes can be characterized within the  
284 proposed framework using  $\Delta = 0$ ; typically  $\mu_1 \ll \mu_0$  but we do not need this  
285 assumption. For simplicity and without loss of generality we neglect high  
286 occupancy vehicles (who do not pay the toll to use the HOT lane) in this  
287 analysis. The reader can verify using Fig. 3 that in this case  $w_1(T_0) = 0$ ,  
288 and therefore the boundary condition (10a) changes to:

$$289 \quad \pi(t_0) = 0, \quad \pi(T_0) = 0. \quad (15)$$

290 We now show that when the pricing strategy is linear, as defined momentarily,  
 291 we can obtain closed-form expressions for revenue, delay and flows. It  
 292 turns out that these quantities are all linear functions of a single parameter,  
 293 which makes the optimization of this system very simple, to the point where  
 294 the appropriate pricing strategy to accomplish a given objective is reduced  
 295 to choosing a single parameter value.

296

297 *Definition:* We say that tolls are linear in the arrivals if there is a constant,  
 298  $a$ , called the pricing coefficient, such that:

$$299 \quad \dot{\pi}(t) = (\rho(t) - 1) a, \quad t_0 \leq t \leq T_0, \quad (16)$$

300 or equivalently (letting  $t_0 = 0$ ),

$$301 \quad \pi(t) = (A(t) - \mu t) a / \mu, \quad t_0 \leq t \leq T_0, \quad (17)$$

302 which means that the toll is proportional to the system queue at  $t$ ,  $A(t) - \mu t$ ,  
 303 or delay  $w(t) = (A(t) - \mu t) / \mu$ ; see Fig. 3a. Notice that  $a$  is dimensionless.  
 304 This strategy is “real-time” because from (16) it is clear that to determine  
 305 the toll at time  $t$  all that is needed is the demand-capacity ratio at the same  
 306 time, which can be measured in real-time.

307 **Result 4.1.** (Assignment, delays and revenues under linear tolls) *Under lin-*  
 308 *ear pricing the flow assigned to each alternative, delays and revenue are linear*  
 309 *functions of the pricing coefficient; i.e., in dimensionless form:*

$$310 \quad \rho_0(a, t) = (1 + a\bar{\mu}_1)\rho(t) - a\bar{\mu}_1, \quad t_0 \leq t \leq T_0, \quad (18a)$$

$$311 \quad \rho_1(a, t) = (1 - a\bar{\mu}_0)\rho(t) + a\bar{\mu}_0, \quad t_0 \leq t \leq T_0, \quad (18b)$$

$$312 \quad W_0(a)/W = (1 + a\bar{\mu}_1)\bar{\mu}_0, \quad (18c)$$

$$313 \quad W_1(a)/W = (1 - a\bar{\mu}_0)\bar{\mu}_1, \quad (18d)$$

$$314 \quad R(a)/W = a\bar{\mu}_1. \quad (18e)$$

316 **Proof** For the flow assigned to each alternative, combining (8) and (16) gives  
 317 the desired result. For the delays, we notice that on alternative  $r$  it is given  
 318 by (11b) using  $\int_{t_0}^{T_0} \pi(t)dt = aW/\mu$ , which follows from (17), and simplifies  
 319 to (18c) and (18d) as sought. In the case of the revenue, from Result 3.1 the

320 revenue is proportional to  $\int_{t_0}^{T_0} \lambda(t)\pi(t)dt$ , which integrated by parts gives:

$$321 \quad \int_{t_0}^{T_0} \lambda(t)\pi(t)dt = A(t)\pi(t)|_{t_0}^{T_0} - \int_{t_0}^{T_0} A(t)\dot{\pi}(t)dt \quad (19a)$$

$$322 \quad = a \int_{t_0}^{T_0} A(t)(1 - \lambda(t)/\mu)dt \quad (19b)$$

$$323 \quad = a \left( \int_{t_0}^{T_0} A(t)dt - \frac{1}{2}A(T_0)T_0 \right) \quad (19c)$$

$$324 \quad = aW \quad (19d)$$

326 The first term in (19a) is zero because of (15), while (19c) results from  
 327  $\int A(t)\lambda(t)dt = A(t)^2/2$  and noting that  $A(T_0) = \mu T_0$ . The revenue is ob-  
 328 tained by substituting (19d) into (13), which gives (18e).  $\square$

329 It is interesting to note that all relevant measures of performance in our  
 330 problem are not only a linear function of a single parameter,  $a$ , but also linear  
 331 functions of all the constants that define the problem:  $\bar{\mu}_0, \bar{\mu}_1$  and  $W$ .

332 Imposing nonnegative delays gives the bounds for the pricing coefficient:

$$333 \quad a_{\max} = 1/\bar{\mu}_0, \quad a_{\min} = -1/\bar{\mu}_1, \quad (20)$$

334 which also can be derived by imposing  $\rho_0(t) \geq 1$  for  $a_{\min}$  and  $\rho_1(t) \geq 1$  for  
 335  $a_{\max}$ . Since the revenue is a linearly increasing function of  $a$ , it follows that  
 336 the maximum revenue is  $R(a_{\max})$ , namely:

$$337 \quad R_{\max} = \frac{\mu_1}{\mu_0}W. \quad (21)$$

338 Replacing  $a = a_{\max}$  in (18) shows that maximum revenue implies the HOT  
 339 lane is used at capacity with no queues.

#### 340 4.1. Optimizing operator objectives

341 Since all performance measures become analytical under linear pricing, it  
 342 is a simple matter to optimize any particular objective set by the operator.  
 343 For example, it follows from Result 4.1 that any objective function  $f(\cdot)$  that  
 344 is a linear combination of delays and revenue, e.g.:

$$345 \quad f(a) = c_0W_0(a) + c_1W_1(a) + R(a), \quad \text{with } c_0, c_1 = \text{constants}, \quad (22)$$

346 is also a linear function of the pricing coefficient. Therefore, the optimal  
 347 solution will be either  $a_{\min}, a_{\max}$  or an arbitrary value within these bounds,  
 348 depending on the sign of  $f'(a) = \bar{\mu}_1 W(1 + \bar{\mu}_0(c_0 - c_1))$ . Of course, nonlinear  
 349 objectives are also possible but the optimum reduces to finding the extremum  
 350 of a scalar function.

351 Another type of objective could be maximizing revenue while ensuring  
 352 that the GPL delay does not exceed the HOT lane delay by a factor of,  
 353 say,  $r$ ; i.e.:  $\max_a R(a)$  subject to  $W_0(a) \leq rW_1(a)$ . Since  $R(a)$  is a linearly  
 354 increasing function of  $a$ , the optimum  $a$ , namely  $a^*$ , is the highest possible  
 355 value of  $a$ , which in this case is given by the condition  $W_0(a^*) = rW_1(a^*)$ , or:

$$356 \quad a^* = \frac{\mu_1 r - \mu_0}{\mu_0 \bar{\mu}_1 (1 + r)}, \quad (23)$$

357 provided that it is not larger than  $a_{\max} = 1/\bar{\mu}_0$ . The corresponding revenue  
 358  $R(a^*)$  is given by (18e), which can be written as  $R(a^*) = (r - \mu_0/\mu_1)/(1 +$   
 359  $r)R_{\max}$ . This implies that under this policy, revenue decreases by a factor of  
 360  $(1 + r)/(r - \mu_0/\mu_1)$  compared to the maximum revenue policy.

#### 361 4.2. Other real-time pricing strategies

362 It turns out that a wide family of real-time pricing strategies that may  
 363 arise in practice are linear in the arrivals and therefore share the properties  
 364 outlined in the preceding section. In these strategies, tolls are calculated as  
 365 linear functions of the traffic conditions on (i) the HOT lane, (ii) the GPL,  
 366 and/or (iii) all lanes. The appendix shows this when the traffic condition is  
 367 the delay or the number of vehicles in queue, and Table 1 summarizes the  
 368 results.

369 This result extends to any traffic condition that is a linear function of  
 370 the delay in each alternative  $w_r(t)$ . They include the number of vehicles in  
 371 the queue  $\mu_r w_r(t)$ , travel time  $\tau_r + w_r(t)$ , pace  $(\tau_r + w_r(t))/L$ , density  $k(t) =$   
 372  $k_c + \mu_r w_r(t)/L$ ; if we assume a linear congestion branch in the flow-density  
 373 relationship one may also include the flow in congestion  $q(t) = (\kappa - k(t))w$ ,  
 374 where  $\kappa$  is the jam density and  $-w$  is the wave speed. The only difference  
 375 is the way each one would be implemented in practice. Each strategy would  
 376 keep track of different traffic variables, such as queue length, delay, density,  
 377 etc. An operator should choose to track the traffic variables that can be  
 378 measured more accurately with the available technology. In most cases, it  
 379 is more reliable to estimate speeds so that a delay-based strategy may be  
 380 advisable.

381 *4.3. Numerical example*

382 To illustrate our method, consider the HOT problem with the parameter  
383 values shown in Fig.7. Tolls are given by (17) and the traffic assignment by  
384 (18a), (18b). Fig.7 illustrate the cases  $a = a_{\max}$  and  $a$  given by (23), which  
385 correspond to the scenario of maximum revenue under no constraints, and  
386 constrained such that the GPL delay does not exceed the HOT lane delay by a  
387 factor of  $r = 5$ , respectively. It can be seen that in the unconstrained scenario,  
388 the GPL users experience all the delay while HOT users enjoy no queues,  
389 as expected. In contrast, in the constrained scenario both alternatives are  
390 congested with  $W_0/W_1 = 5$ , and the revenue decreases by a factor of 6,  
391 as expected. Notice in part e of the figure that the system input-output  
392 diagram for both scenarios is identical, which illustrates that two different  
393 pricing strategies yield the same SO solution.

394 **5. Discussion**

395 As stated in the introduction, our definition of social costs does not in-  
396 clude the effects that tolls may have on trip generation or departure-time  
397 choice. This does not mean that demand is considered inelastic here, at  
398 least in the traditional sense: demand is assumed inelastic for each particu-  
399 lar rush hour (because users do not know the toll in advance), but next day  
400 demand may change due to pricing. In particular, we provided an answer  
401 to the question: given the current state of the system, what is the toll that  
402 minimizes total system delay until the end of the rush hour? This approach  
403 allowed the closed-form solutions and insights derived here, and it may not  
404 be far-fetched: empirical results concerning departure time variations due  
405 to dynamic pricing on managed lanes that have and untolled alternative are  
406 mixed (Ozbay et al., 2006; Lam and Small, 2001).

407 Not surprisingly, our findings differ sharply from the classical result in the  
408 congestion pricing literature that the SO solution is unique with the tolled  
409 facility always queue-free. This result applies for both the (i) departure-  
410 time choice literature (see e.g., Vickrey, 1969; Arnott et al., 1990; Braid,  
411 1996) and the (ii) static assignment literature that explicitly includes cost  
412 elasticity (see e.g., Verhoef et al., 1996; Liu and McDonald, 1998; Small and  
413 Yan, 2001; Verhoef and Small, 2004). If the framework proposed here is  
414 supplemented with a departure-time and/or cost elasticity component for  
415 day-to-day demand variations it remains to be seen if the solution presented

416 here becomes unique and queue-free in the long run. This is currently being  
 417 investigated by the authors.

418 Similarly as in section 3.3, it can be shown that the social (delay) benefits  
 419 of SO tolling compared to no tolling in the case  $\Delta < 0$  are bounded by  
 420  $(T - \tau_0)|\Delta|\bar{\mu}_0$ . It follows that the only case where SO pricing does not provide  
 421 social benefit is when  $\Delta = 0$ . In any case, SO tolls have the advantage of  
 422 providing a revenue source and giving flexibility to the operator where to store  
 423 the queues, while keeping system costs at a minimum. User costs, however,  
 424 increase with SO pricing since tolls have the effect of increasing user costs in  
 425 both alternatives. To see this, note that for ML users the variable part of the  
 426 total user cost is  $W_1(\pi) + R(\pi)$ , and for GP users it is  $W_0(\pi)$ ; see Fig. 3b,c.  
 427 In the case  $\Delta = 0$  we can use (18) to show that user costs are linear in  $a$ , i.e.  
 428  $W_0 = (1 + a\bar{\mu}_1)\bar{\mu}_0W$  and  $W_1 + R = (1 + a\bar{\mu}_1)\bar{\mu}_1W$ , which shows that user  
 429 costs in both alternatives increase with revenue  $R = a\bar{\mu}_1$ .

430 The concept of marginal costs for an alternative needs some clarification  
 431 as it becomes ambiguous when capacity is reached, i.e. the left and right  
 432 derivatives of the cost function are different. This happens in our problem  
 433 starting at time  $t_1$  when the ML is first used at capacity and until time  $t_0$ . It  
 434 can be seen in Fig. 4a that during this time interval an extra vehicle to the  
 435 ML would induce a jump in the marginal cost curve from dashed segment  
 436 “3” to “4” in the figure (right derivative), whereas one fewer vehicle to this  
 437 alternative would keep the marginal cost constant at  $\tau_1$  (left derivative). Dis-  
 438 ambiguity can pose some difficulty when implementing the congestion pricing  
 439 principle. But this paper has shown that the left derivative is the only one  
 440 consistent with the desired SO flow pattern.

441 Linear pricing strategies, as defined in this paper, are intuitive to ap-  
 442 ply in practice and exhibit appealing properties. They allowed us to derive  
 443 analytical expressions for all variables of interest for HOT lanes, including  
 444 revenues and total delay in each alternative, which are linear functions of a  
 445 single parameter, the pricing coefficient  $a$ . How to determine this param-  
 446 eter depends on the operator’s objective, as outlined in section 4.1. Note  
 447 that Pareto efficient and/or equitable pricing strategies could be devised in  
 448 a similar fashion, and this is currently being investigated by the authors. To  
 449 implement this strategy all the operator has to do is start charging when tot-  
 450 al demand exceeds total capacity, and apply (16) until the end of the rush.  
 451 This mechanism only requires measuring total system demand in real-time,  
 452 which will vary stochastically and does not need to be known in advance.  
 453 Linear pricing may be applied when  $\Delta \neq 0$  but only up to the time when the

454 active bottleneck restriction is hit; see e.g. the semi-linear strategy in Fig. 5.

455 The results from section 3 also apply to the case  $\Delta < 0$  if one interchanges  
456  $t_1$  and  $t_0$ , and also  $T_1$  and  $T_0$ ; see Fig. 8. It can be seen from the figure that  
457 negative tolls may be necessary to ensure SO, which can be implemented  
458 as a credit to ML users. In this case too, maximizing revenue is equivalent  
459 to maximizing the difference between GPL delay and ML delay. Therefore,  
460 maximum revenue is achieved by eliminating queues from the ML facility  
461 while remaining at capacity, up to time  $T_1$  when the facility is no longer  
462 used. This differs from the case  $\Delta > 0$ , where one has to allow congestion in  
463 both alternatives at  $T_0$ . In any case, except for these nuances at the end of  
464 the rush, this maximum revenue strategy coincides with common practice,  
465 where the toll is set to guarantee a free-flow ML facility. It has to be noted,  
466 however, that there are other non-SO strategies that would generate even  
467 more revenue, but at the expense of a greater total delay.

468 Finally, it is worth noting that a natural extension of this framework  
469 would be to incorporate driver heterogeneity. The linearity property un-  
470 veiled in section 4 could be exploited for analyzing driver differences in the  
471 willingness to pay. In our formulation, if drivers' value-of-time is a random  
472 variable, so is the pricing coefficient  $a$ . The conjecture is that Result 4.1 is  
473 still valid replacing  $a$  by its expected value, for the expected values of flows,  
474 delays and revenue. In the same direction, one might want to incorporate  
475 a discrete choice model to capture the effects of income and other socioeco-  
476 nomic variables (e.g., Wu et al., 2012). Subsequently, the SO will maximize  
477 the expected utility rather than total delay as in this paper. It remains open  
478 whether the conclusions obtained in this paper still stand, another topic for  
479 our future investigation.

## 480 **Acknowledgments.**

481 This research was supported by STRIDE/GDOT research project 2012-  
482 089S, and by CEDEUS, CONICYT/FONDAP 15110020. The authors would  
483 like to thank two anonymous referees and the Associate Editor for their  
484 valuable comments and suggestions, which greatly improved this paper.

## 485 **References**

486 Arnott, R., de Palma, A., Lindsey, R., 1990. Departure time and route choice  
487 for the morning commute. *Transportation Research Part B* 24 (3), 209–228.

- 488 Braid, R. M., 1996. Peak-load pricing of a transportation route with and  
489 unpriced substitute. *Journal of Urban Economics* 40 (2), 179–197.
- 490 Burris, M. W., Appiah, J., 2004. Examination of houstons quickride partic-  
491 ipants by frequency of quickride usage. *Transportation Research Record*  
492 1864, 22–30.
- 493 Burris, M. W., Stockton, B. R., 2004. Hot lanes in houston-six years of  
494 experience. *Journal of Public Transportation* 7 (3), 1–21.
- 495 Burris, M. W., Ungemah, D. H., Mahlawat, M., Pannu, M. S., 2009. Investi-  
496 gating the impact of tolls on high-occupancy-vehicle lanes using managed  
497 lanes. *Transportation Research Record* 2065, 113–122.
- 498 Carey, M., Watling, D., 2012. Dynamic traffic assignment approximating the  
499 kinematic wave model: System optimum, marginal costs, externalities and  
500 tolls. *Transportation Research Part B* 46 (5), 634–648.
- 501 Finkleman, J., Casello, J., Fu, L., 2011. Empirical evidence from the greater  
502 toronto area on the acceptability and impacts of hot lanes. *Transport Pol-*  
503 *icy* 18 (6), 814–824.
- 504 Kuwahara, M., 2007. A theory and implications on dynamic marginal cost.  
505 *Transportation Research Part A* 41 (7), 627 – 643.
- 506 Lam, T. C., Small, K. A., 2001. The value of time and reliability: measure-  
507 ment from a value pricing experiment. *Transportation Research Part E*  
508 37 (2-3), 231 – 251, advances in the Valuation of Travel Time Savings.  
509 URL <http://www.sciencedirect.com/science/article/pii/S1366554500000168>
- 510 Laval, J., Daganzo, C., 2006. Lane-changing in traffic streams. *Transporta-*  
511 *tion Research Part B* 40 (3), 251–264.
- 512 Laval, J. A., 2009. Graphical solution and continuum approximation for the  
513 single destination dynamic user equilibrium problem. *Transportation Re-*  
514 *search Part B* 43 (1), 108–118.
- 515 Li, J., 2001. Explaining high-occupancy-toll lane use. *Transportation Re-*  
516 *search Part D* 6 (1), 61–74.



- 517 Li, J., Govind, S., 2002. An optimization model for assessing pricing strate-  
518 gies of managed lanes. No. 03-2082. Proc., 82nd Annual Meeting of the  
519 Transportation Research Board.
- 520 Liu, L. N., McDonald, J. F., 1998. Efficient congestion tolls in the presence  
521 of unpriced congestion: A peak and off-peak simulation model. *Journal of*  
522 *Urban Economics* 44 (3), 352–366.
- 523 Lou, Y., Yin, Y., Laval, J. A., 2011. Optimal dynamic pricing strategies for  
524 high-occupancy/toll lanes. *Transportation Research Part C* 19 (1), 64–74.
- 525 Muñoz, J. C., Laval, J. A., 2005. System optimum dynamic traffic assignment  
526 graphical solution method for a congested freeway and one destination.  
527 *Transportation Research Part B* 40 (1), 1–15.
- 528 Ozbay, K., Yanmaz-Tuzel, O., Holgun-Veras, J., 2006. Evaluation of com-  
529 bined traffic impacts of time-of-day pricing program and e-zpass usage on  
530 new jersey turnpike. *Transportation Research Record* 1960, 40–47.
- 531 Podgorski, K. V., Kockelman, K. M., 2006. Public perception of toll roads: A  
532 survey of the texas perspective. *Transportation Research Part A* 40 (10),  
533 888–902.
- 534 Small, K. A., Yan, J., 2001. The value of "value pricing" of roads: Second-  
535 best pricing and product differentiation. *Journal of Urban Economics*  
536 49 (2), 310–336.
- 537 Supernak, J., Golob, J., Golob, T. F., Kaschade, C., Kazimi, C., Schreffler,  
538 E., Steffey, D., 2002a. San Diegos interstate 15 congestion pricing project:  
539 Attitudinal, behavioral, and institutional issues. *Transportation Research*  
540 *Record* 1812, 78–86.
- 541 Supernak, J., Golob, J., Golob, T. F., Kaschade, C., Kazimi, C., Schreffler,  
542 E., Steffey, D., 2002b. San Diegos interstate 15 congestion pricing project:  
543 Traffic-related issues. *Transportation Research Record* 1812, 43–52.
- 544 Supernak, J., Steffey, D., Kaschade, C., 2003. Dynamic value pricing as in-  
545 strument for better utilization of high-occupancy toll lanes. *Transportation*  
546 *Research Record* 1839, 55–64.

- 547 Verhoef, E., Nijkamp, P., Rietveld, P., 1996. Second-best congestion pricing:  
548 The case of an untolled alternative. *Journal of Urban Economics* 40 (3),  
549 279–302.
- 550 Verhoef, E. T., Small, K. A., 2004. Product differentiation on roads: Con-  
551 strained congestion pricing with heterogeneous users. *Journal of Transport*  
552 *Economics and Policy* 38 (1), 127–156.
- 553 Vickrey, W. S., May 1969. Congestion theory and transport investment.  
554 *American Economic Review*, American Economic Association 59 (2), 251–  
555 60.
- 556 Wu, D., Yin, Y., Lawphongpanich, S., H, Y., 2012. Design of more equitable  
557 congestion pricing and tradable credit schemes for multimodal transporta-  
558 tion networks. *Transportation Research Part B* 46 (9), 1273–1287.
- 559 Yin, Y., Lou, Y., 2009. Dynamic tolling strategies for managed lanes. *Journal*  
560 *of Transportation Engineering* 135 (2), 45–52.
- 561 Zhang, G., Wang, Y., Wei, H., Yi, P., 2008. A feedback-based dynamic  
562 tolling algorithm for high-occupancy toll lane operations. *Transportation*  
563 *Research Record* 2065, 54–63.
- 564 Zhang, G., Yan, S., Wang, Y., 2009. Simulation-based investigation on high-  
565 occupancy toll lane operations for washington state route 167. *Journal of*  
566 *Transportation Engineering* 135 (10), 677–686.
- 567 Zmud, J., Bradley, M., Douma, F., Simek, C., 2007. Attitudes and willing-  
568 ness to pay for tolled facilities: a panel survey evaluation. *Transportation*  
569 *Research Record* 1996, 58–65.

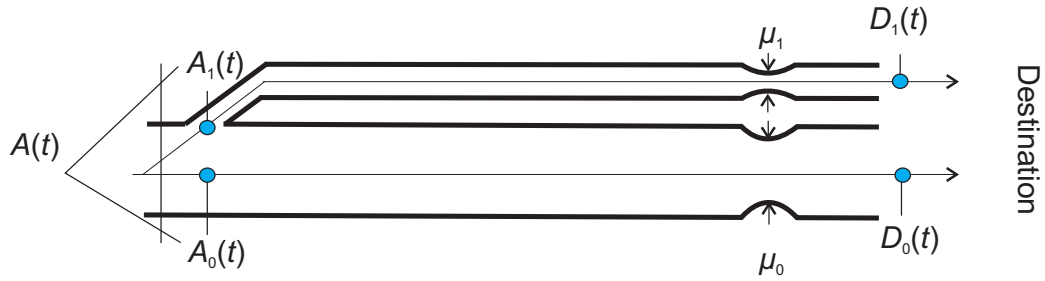


Figure 1: Schematic representation of the network.

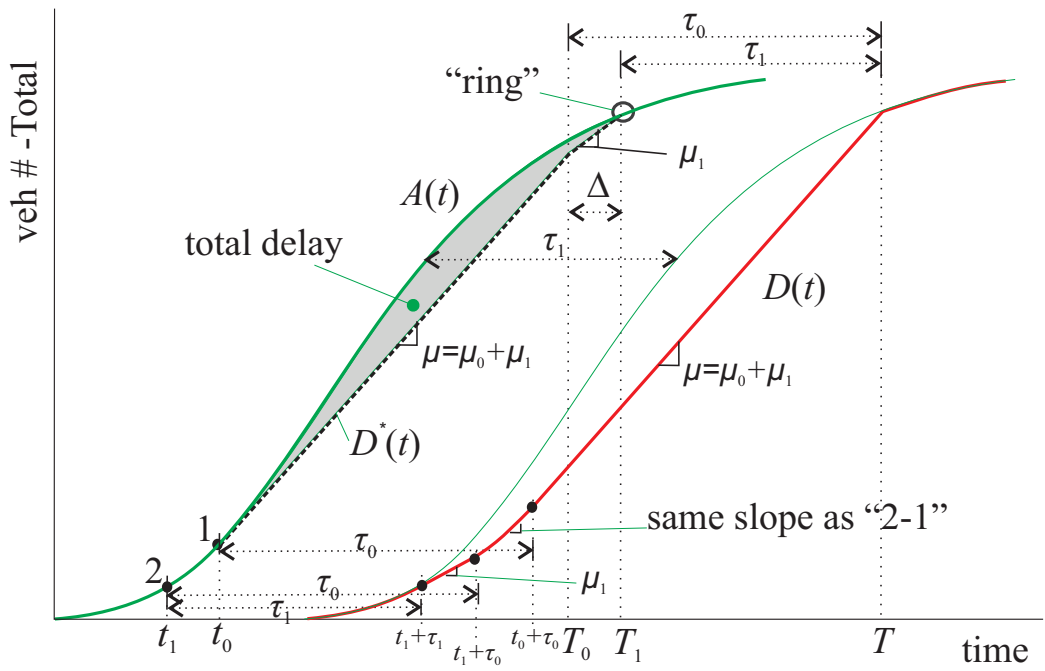


Figure 2: System Optimum input-output diagram.

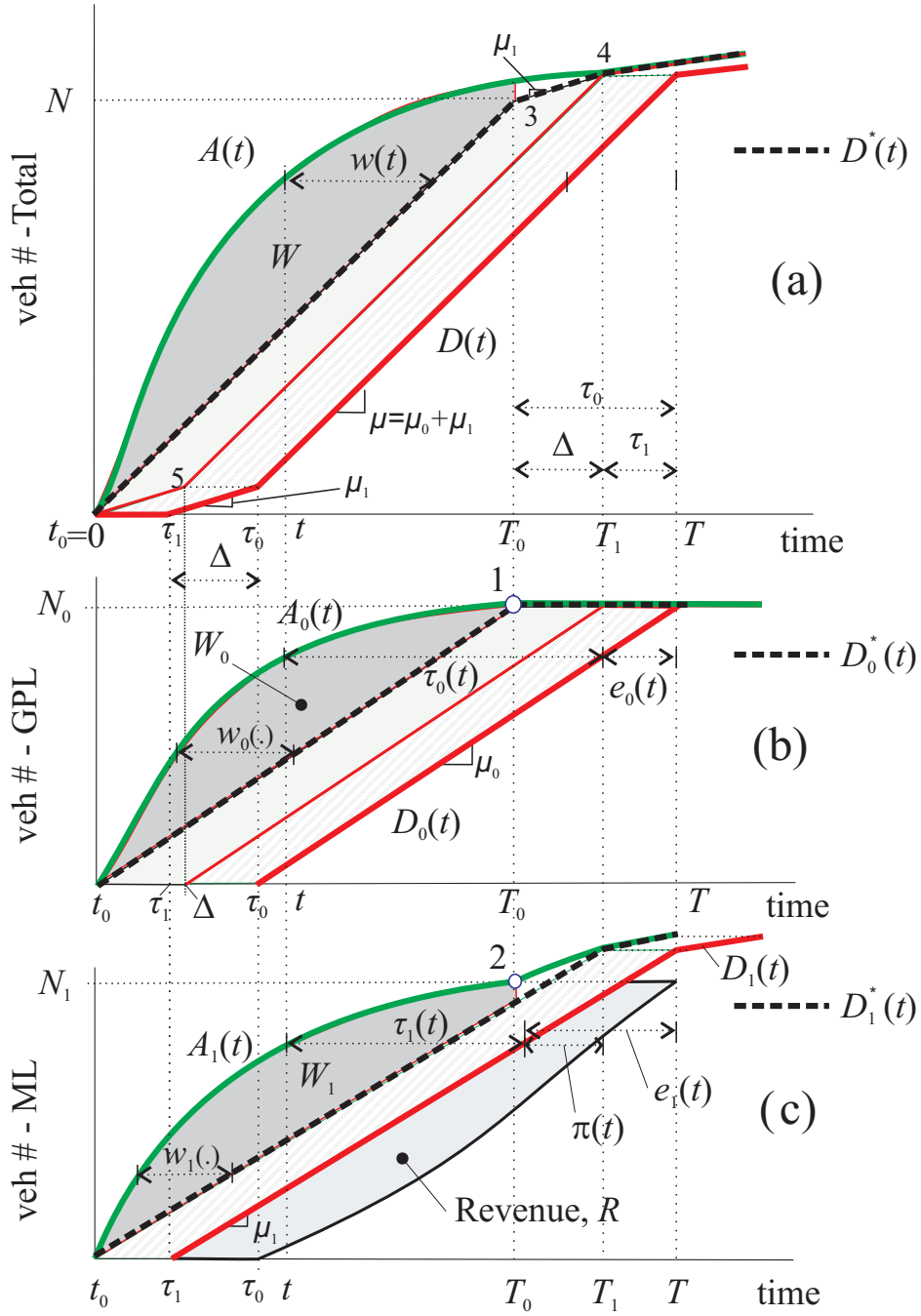


Figure 3: System Optimum input-output diagram for users arriving at  $t \geq t_0$ .

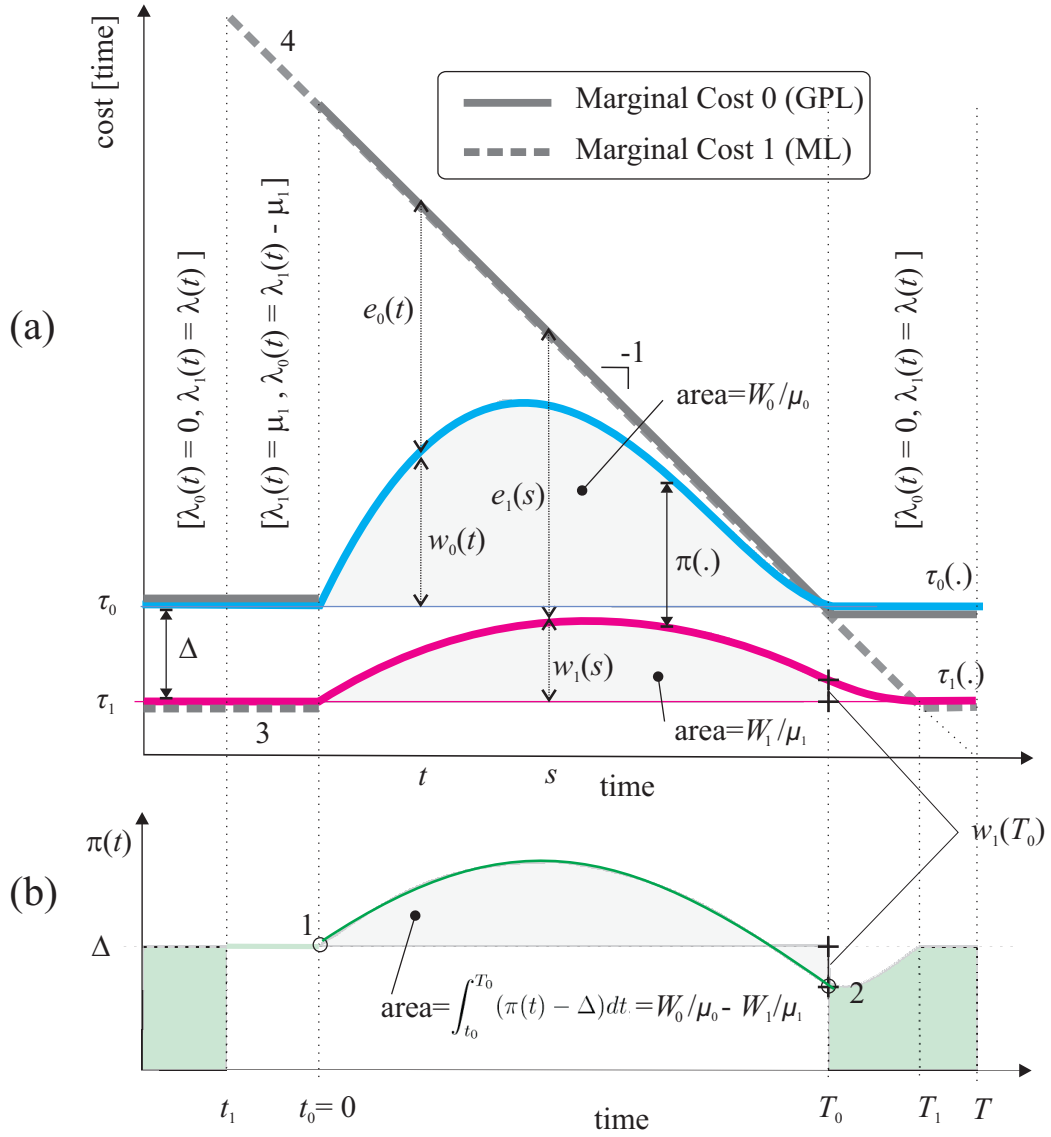


Figure 4: Evolution of the system (a) marginal cost, externality, travel time and (b) toll. The shaded rectangles in (b) indicate that the toll could be anywhere inside this area.

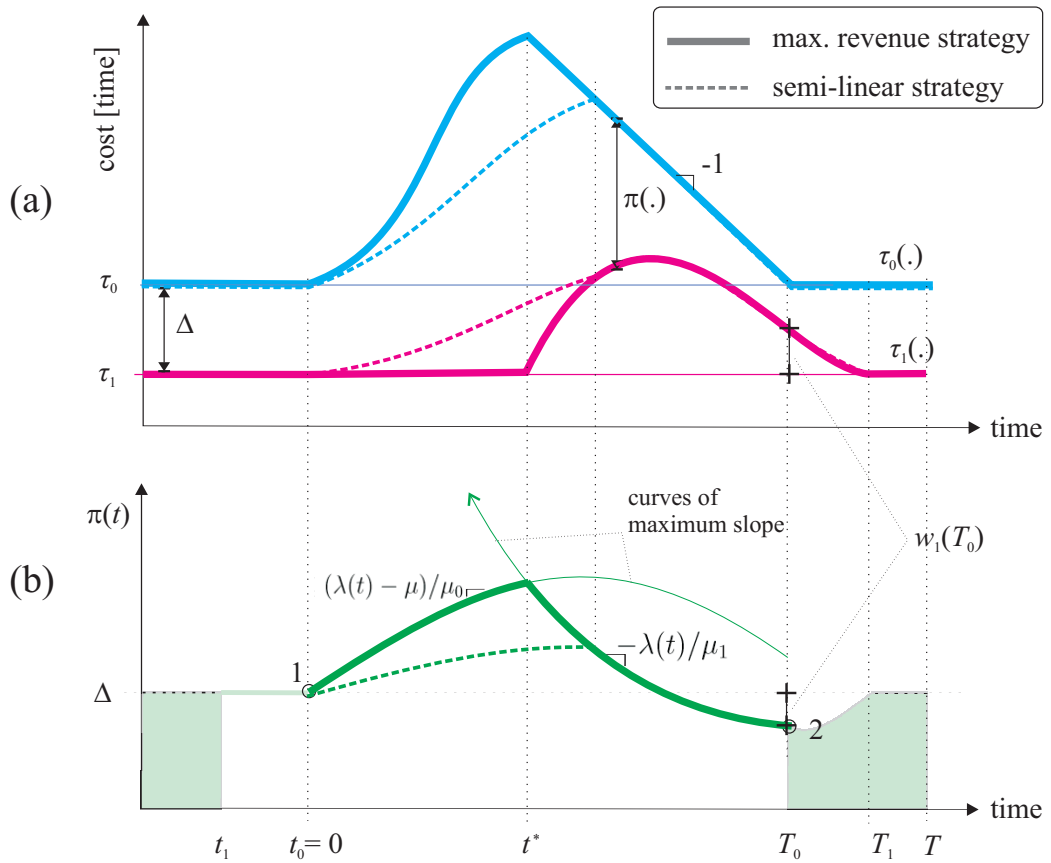


Figure 5: Toll of maximum revenue.

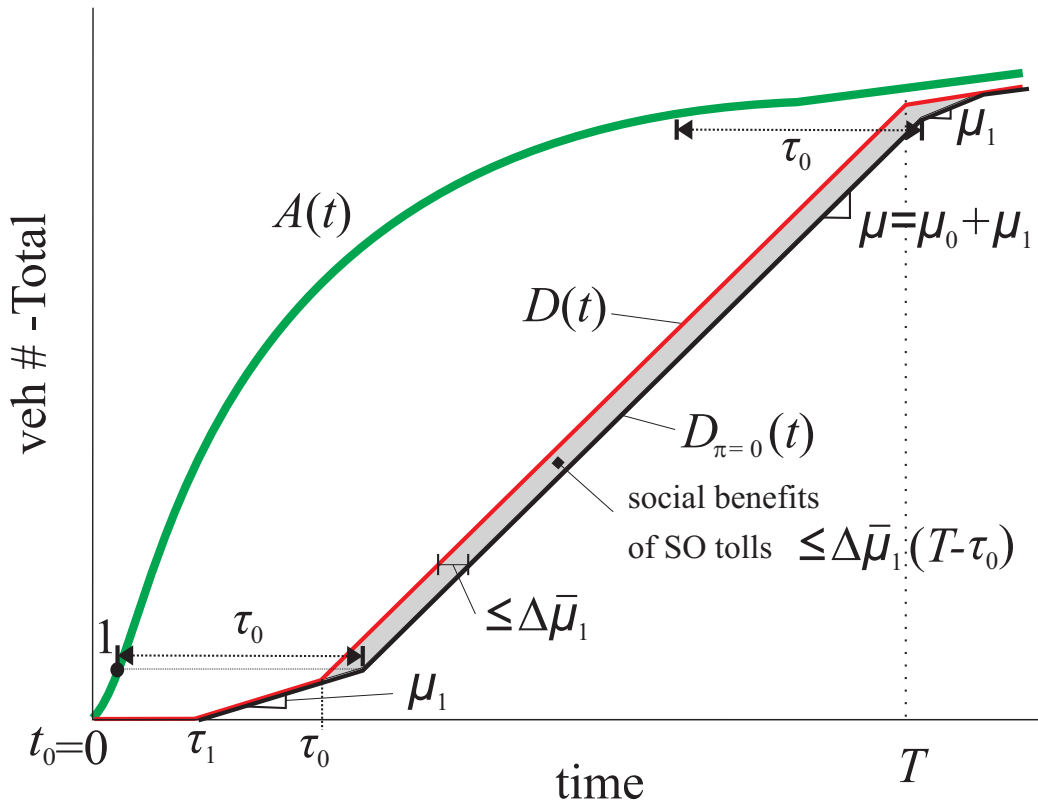


Figure 6: Input-output diagram showing the delay benefits of SO tolling compared to no tolling; case  $\Delta > 0$ .

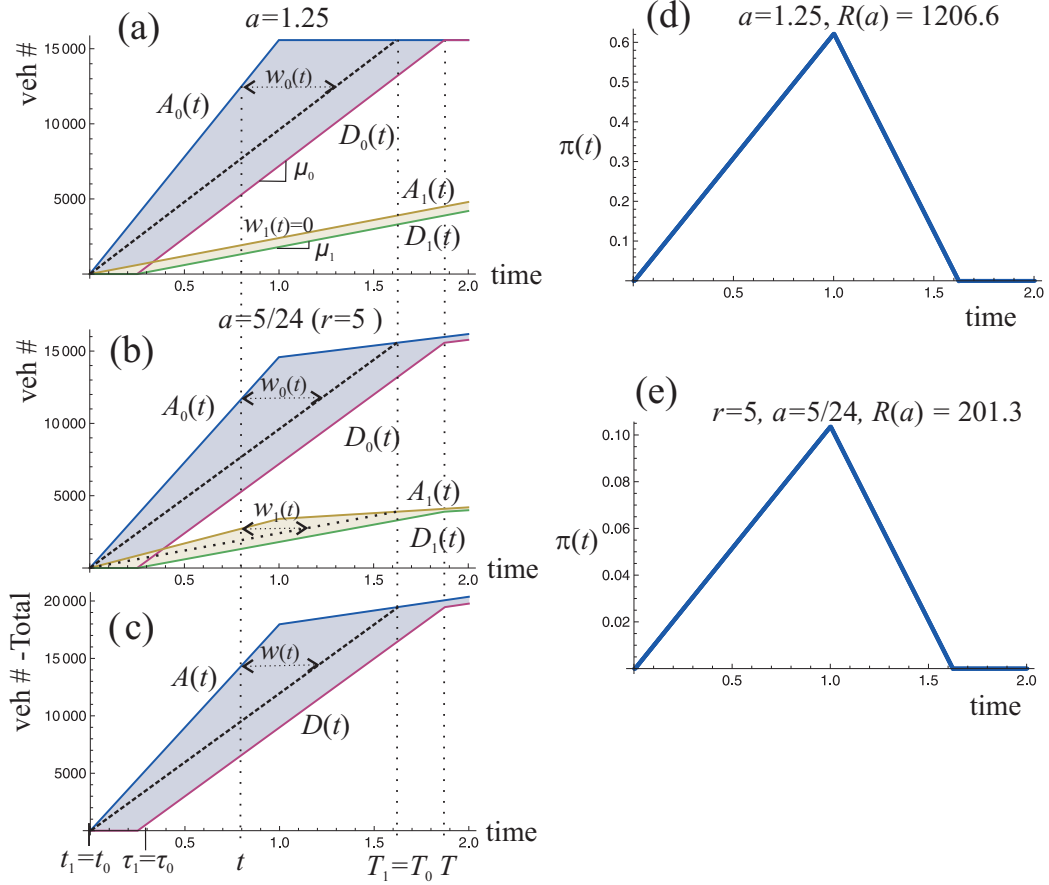


Figure 7: Numerical example. Parameter values:  $\mu_0=9,600$  vph,  $\mu_1=2,400$  vph,  $\tau_0 = \tau_1 = 0.25$  hr ( $\Delta=0$ ); the arrival rate  $\lambda(t)$  is 18,000 vph in  $0 < t < 1$  hr, and 2,400 vph in  $t > 1$  hr, where  $t_1 = t_0 = 0$ hr. (a) input-output diagram for scenario of maximum revenue under no constraints, where  $a_{\max} = 1.25$  from (20); (b) input-output diagram for scenario of maximum revenue constrained so that the GPL delay does not exceed the HOT lane delay by a factor of  $r = 5$ , respectively, where  $a = a^* = 5/24$  given by (23); (c) system input-output diagram; (d) and (e) give the toll corresponding to (a) and (b).



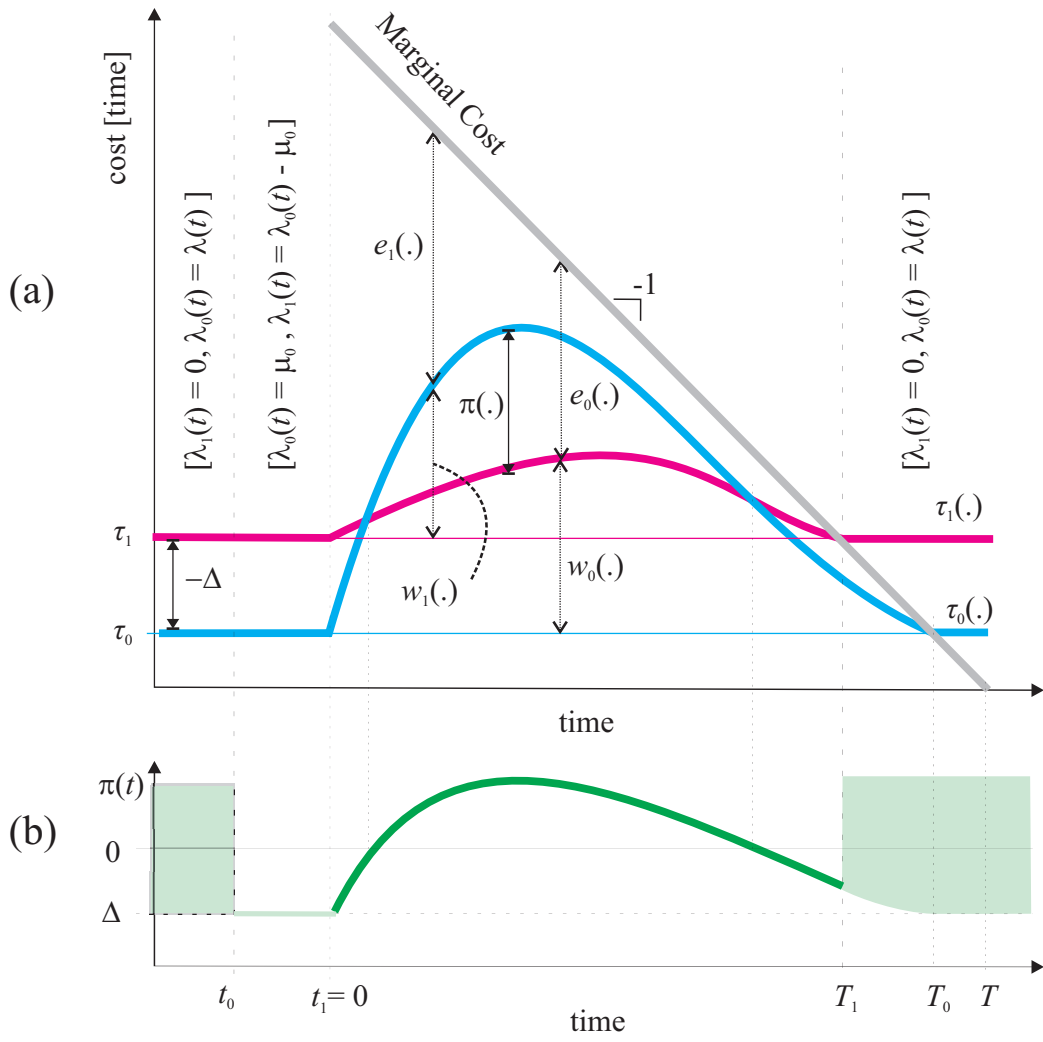


Figure 8: Evolution of the system when  $\Delta < 0$ : (a) marginal cost, externality, travel time and (b) toll. The shaded rectangles in (b) indicate that the toll could be anywhere inside this area.

Table 1: Pricing Strategies summary

Toll linear in	$\pi(t)$	$\lambda_0(t)/\mu_0$	$C_{\min}$	$C_{\max}$	$a$
ML queue	$c(A_1(t) - \mu_1 t)$	$\frac{\lambda(t) + c\mu_1(\lambda(t) - \mu_1)}{\mu + c\mu_0\mu_1}$	$-\frac{\mu}{\mu_1(\mu_0 + \mu\mu_1)}$	$\infty$	$\frac{c\mu_1\mu}{\mu + c\mu_0\mu_1}$
GPL queue	$c(A_0(t) - \mu_0 t)$	$\frac{\lambda(t) - c\mu_0\mu_1}{\mu - c\mu_0\mu_1}$	$-\frac{\mu}{(\mu-1)\mu_0\mu_1}$	$1/\mu_0$	$\frac{c\mu\mu_0}{\mu - c\mu_0\mu_1}$
Queue on All lanes	$c(A(t) - \mu t)$	$\frac{\lambda(t) + c(\lambda(t) - \mu)\mu_1}{\mu}$	$-1/\mu_1$	$1/\mu_0$	$c\mu$
ML delay	$c\left(\frac{A_1(t)}{\mu_1} - t\right)$	$\frac{\lambda(t)(1+c) - c\mu_1}{\mu + c\mu_0}$	$-\frac{\mu}{\mu_0 + \mu\mu_1}$	$\infty$	$\frac{c\mu}{\mu + c\mu_0}$
GPL delay	$c\left(\frac{A_0(t)}{\mu_0} - t\right)$	$\frac{\lambda(t) - c\mu_1}{\mu - c\mu_1}$	$-\frac{\mu}{(\mu-1)\mu_1}$	$1$	$\frac{c\mu}{\mu - c\mu_1}$
Delay on All lanes	$c\left(\frac{A(t)}{\mu} - t\right)$	$\frac{\mu_0(\lambda - c\mu_1) + \mu_1(\lambda + c(\lambda - \mu_1))}{\mu^2}$	$-\frac{\mu}{\mu_1}$	$\frac{\mu}{\mu_0}$	$c$

570 **Appendix A. Comparison of Real-Time Pricing Strategies on HOT**  
571 **lanes**

572 This appendix shows that strategies where tolls are calculated as linear  
573 functions of the (a) delay or (b) the number of vehicles in queue on (i) the  
574 HOT lane, (ii) the GPL, and/or (iii) all lanes, are linear in the arrivals and  
575 therefore are in fact mathematically equivalent. Since the methodology is  
576 identical in all cases, we illustrate the analysis for one strategy, case (b)(i)  
577 above, and summarize all results in Table 1.

578 *Toll linear in the queue on the HOT lane*

579 The queue on the HOT lane at time  $t$  is  $A_1(t) - \mu_1 t$ , and therefore under  
580 this strategy we have:

$$581 \quad \pi(t) = (A_1(t) - \mu_1 t) c, \quad t_0 \leq t \leq T_0, \quad (\text{A.1})$$

582 where  $c$  is a constant that involves the value of time and has units of time in  
583 this case. To obtain the UE assignment under this strategy we substitute

$$584 \quad \dot{\pi}(t) = (\lambda_1(t) - \mu_1) c \quad (\text{A.2})$$

585 in (8a) and (8b), which leads to

$$586 \quad \lambda_0(t) = \mu_0 \frac{\lambda(t) + c\mu_1(\lambda(t) - \mu_1)}{\mu + c\mu_0\mu_1} \quad (\text{A.3a})$$

$$587 \quad \lambda_1(t) = \lambda(t) - \lambda_0(t) = \mu_1 \frac{\lambda(t) + c\mu_0\mu_1}{\mu + c\mu_0\mu_1} \quad (\text{A.3b})$$

589 Combining (A.2) and (A.3b) reveals that this strategy is linear in the arrivals  
590 with pricing coefficient  $a = (c\mu_1\mu)/(\mu + c\mu_0\mu_1)$ ; i.e.:

$$591 \quad \dot{\pi}(t) = \left(\frac{\lambda(t)}{\mu} - 1\right) \frac{c\mu_1\mu}{\mu + c\mu_0\mu_1} \quad (\text{A.4})$$

592 To ensure that the SO conditions are met at all times  $t_0 \leq t \leq T_0$ , we  
593 can identify a feasible interval  $c_{\min} \leq c \leq c_{\max}$  similarly as in the main text;  
594 i.e., by imposing  $\rho_0(t) \geq 1$  and  $\rho_1(t) \geq 1$ . Finally, Table 1 summarizes the  
595 results for all the strategies considered in this appendix. Notice that using  
596  $c_{\max}$  and  $c_{\min}$  to evaluate  $a$  in Table 1 gives the same values for all strategies,  
597 and they coincide with (20) as expected.